Dominant role of local-moment interactions in the magnetic ordering of iron pnictide superconductors: A comparative study of arsenides and antimonides from first principles

Chang-Youn Moon, Se Young Park, and Hyoung Joon Choi*
Department of Physics and IPAP, Yonsei University, Seoul 120-749, Korea
(Received 14 February 2009; revised manuscript received 4 June 2009; published 31 August 2009)

The magnetic properties of various iron pnictides are investigated using first-principles pseudopotential calculations. We consider three different families, LaFe*Pn*O, $BaFe_2Pn_2$, and LiFe*Pn* with *Pn*=As and Sb, and find that the Fe local spin moment and the stability of the stripe-type antiferromagnetic phase increases from As to Sb for all of the three families, with a partial gap formed at the Fermi energy. In the meanwhile, the Fermi-surface nesting is found to be enhanced from *Pn*=As to Sb for LaFe*Pn*O but not for $BaFe_2Pn_2$ and LiFe*Pn*. These results indicate that the local-moment interaction is the dominant factor over the Fermi-surface nesting in determining the stability of the magnetic phase in these materials and that the partial gap is an induced feature by a specific magnetic order.

DOI: 10.1103/PhysRevB.80.054522 PACS number(s): 74.70.Dd, 71.15.Mb, 71.18.+y, 75.25.+z

I. INTRODUCTION

The iron pnictide superconductors and their fascinating physical properties have become central issues in many fields since their recent discoveries.[1–3] The prototype materials are REFeAsO with various rare-earth (RE) elements and the superconducting transition temperature (T_c) is as high as 55 K in doped SmFeAsO.[4] Other compounds with various types of insulating layers are also superconducting when doped, such as K-doped $BaFe_2As_2$ (Refs. 5 and 6) and $SrFe_2As_2$ (Refs. 7 and 8) with T_c of 38 K, and LiFeAs with T_c of 16 (Ref. 9) or 18 K.[10,11] Without doping, these materials exhibit a peculiar magnetic structure of a stripe-type antiferromagnetic (AFM) spin-configuration coupled to orthorhombic atomic structure, and either hole or electron doping destroys the AFM and the superconductivity emerges subsequently. Hence the magnetism is considered to be closely related to the superconductivity in these materials[12–16] and the spin-fluctuation-mediated superconductivity is assumed in many theoretical works.[17–19]

Understanding the nature of magnetism in these materials is thus of crucial importance but it still under debate. On one hand, many theoretical[16,20–22] and experimental[22–26] works emphasize on the itinerant nature of the magnetism of the spin-density wave (SDW) type, since the electron and hole Fermi surfaces (FS) are separated by a commensurate nesting vector in iron pnictides, which is further supported by the reduced magnetic moment of about 0.3 μ_B (Refs. 24 and 25) and the energy gap near the Fermi energy (E_F). On the other hand, there are also interpretations based on the Heisenberg-type interaction between localized spin moments.[27–29] In this localized-moment picture, the observed stripe-type AFM ordering results from the frustrated spin configuration with the next-nearest-neighbor exchange interaction (J_2) larger than half of the nearest-neighbor (NN) interaction (J_1). It is difficult to decide on either picture as each description seems to have its own supporting evidences, nevertheless, recent theoretical works suggest more comprehensive view where both pictures are relevant in the magnetism in iron pnictides. The itinerant electrons interact with localized moments[30–32] and the magnetism is at the borderline between localized and itinerant behavior.[33]

Recently, motivated by the great success of the As substitution for P in LaFePO on raising T_c, hypothetical iron antimonide compounds have been studied as candidates for a higher-T_c superconductor by first-principles calculations.[34,35] In these works, Sb substitution for As is found to modify the FS nesting and the magnetic stability significantly. Thus, with more variation in compounds including antimonides, more comprehensive understanding of the nature of magnetism in iron pnictides would be possible through a systematic comparative study dealing with many different types of compounds altogether.

In this paper, we present our density-functional pseudopotential calculations of the electronic and magnetic properties of various iron arsenides and antimonides: LaFe*Pn*O, $BaFe_2Pn_2$, and LiFe*Pn* (*Pn*=As and Sb). We find that there is no systematic trend of FS nesting feature between arsenides and antimonides, whereas the stability and the local Fe spin moment of the magnetic phase increase from arsenides to antimonides for all three types of compounds. This finding indicates the dominant role of the Heisenberg-type interaction in stabilizing the magnetic phases when we consider that the local Fe moment is larger for antimonides with the enhanced Hund's rule coupling due to their larger lattice constants. The fingerprint of itinerant magnetism is also present in our calculations, FS reconstruction and the subsequent formation of a partial gap in the density of states (DOS) at E_F, which should rather be regarded as a secondary effect caused by coupling to more robust ordering of local moments.

II. CALCULATIONAL METHOD AND ATOMIC STRUCTURES

Our first-principles calculations are based on the density-functional theory within the generalized gradient approximation for the exchange-correlation energy functional[36] and the

TABLE I. Calculated structure parameters, DOS at E_f [$N(E_f)$], and Fe magnetic moment (m) of LaFeAsO (LFAO), LaFeSbO (LFSO), $BaFe_2As_2$ (BFA), $BaFe_2Sb_2$ (BFS), LiFeAs (LFA), and LiFeSb (LFS). AFM2 represents the stripe-type AFM phase, as is defined in the text. Both for NM and AFM2 phases, c lattice parameter is taken as the distance of two adjacent Fe layers for easier comparison. z_1 represents the z coordinate of La, Ba, or Li, and z_2 represents that of As or Sb. Iron atoms are located at $z=0.5$ along the c axis.

NM (tetragonal)						
	a (Å)	b (Å)	c (Å)	z_1	z_2	$N(E_f)$
LFAO	3.999	3.999	8.706	0.145	0.640	1.7
LFSO	4.106	4.106	9.311	0.130	0.659	2.9
BFA	3.935	3.935	6.314	0	0.696	1.9
BFS	4.324	4.324	6.315	0	0.708	1.8
LFA	3.767	3.767	5.967	0.173	0.734	2.1
LFS	3.995	3.995	6.266	0.211	0.756	2.6
AFM2 (orthorhombic)						
	a (Å)	b (Å)	c (Å)	z_1	z_2	m (μ_B)
LFAO	5.780	5.693	8.875	0.139	0.654	2.83
LFSO	5.955	5.844	9.542	0.124	0.673	3.13
BFA	5.756	5.590	6.520	0	0.712	2.78
BFS	6.231	5.937	7.246	0	0.722	3.22
LFA	5.482	5.285	6.190	0.171	0.745	2.54
LFS	5.830	5.593	6.528	0.199	0.768	2.95

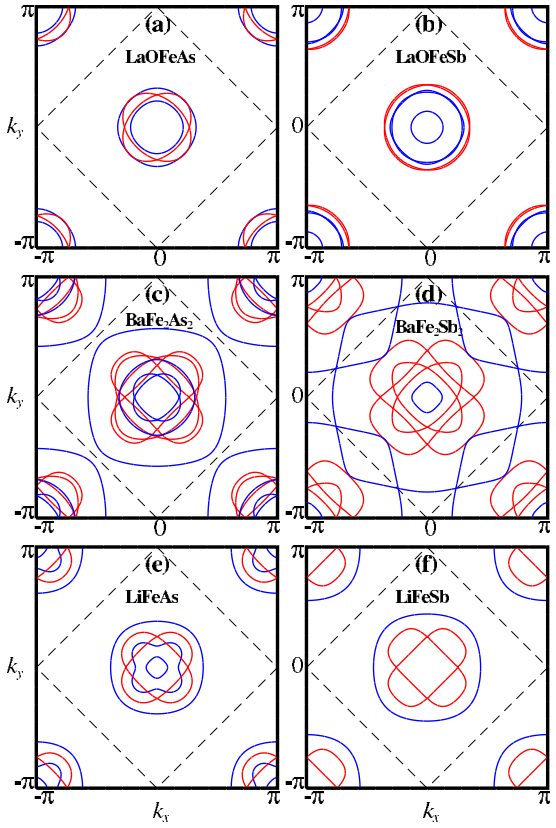

FIG. 1. (Color online) Calculated FS of iron pnictides in the NM phase, drawn in the Brillouin zone of the $\sqrt{2}\times\sqrt{2}$ supercell (dashed lines). Hole pockets are represented in blue (dark gray) and electron pockets are in red (gray). In (c) and (d), the conventional simple tetragonal unit cell is used rather than the primitive body-centered tetragonal unit cell, for easier comparison with other compounds.

ab initio norm-conserving pseudopotentials as implemented in SIESTA code.[37] Semicore pseudopotentials are used for Fe, La, and Ba, and electronic wave functions are expanded with localized pseudoatomic orbitals (double zeta polarization basis set), with the cutoff energy for real-space mesh of 500 Ry. Brillouin-zone integration is performed by Monkhorst-Pack scheme[38] with $12\times12\times6$ k-point grid.

First we obtain the optimized cell parameters and atomic coordinates of compounds by total-energy minimization, as listed in Table I. For the nonmagnetic (NM) phase, tetragonal structures are obtained while the stripe-type AFM phase prefers the orthorhombic structure of the approximate $\sqrt{2}\times\sqrt{2}$ supercell, in agreement with experiments. The lowering of the total energy per Fe atom in the stripe-type AFM phase in the optimized orthorhombic structure relative to the NM phase in the optimized tetragonal unit cell is 354 and 706 meV for LaFeAsO and LaFeSbO, 297 and 745 meV for $BaFe_2As_2$ and $BaFe_2Sb_2$, and 153 and 523 meV for LiFeAs and LiFeSb, respectively. Along with the local magnetic moments on Fe atoms displayed in Table I, this result implies the existence of a universal trend that the magnetism is stronger for antimonides than for arsenides irrespective of the detailed material properties.

III. COMPARISON OF FERMI SURFACES AMONG IRON PNICTIDES

Figure 1 shows the calculated FSs on the $k_z=0$ plane. To facilitate the investigation of the nesting feature, the electron and hole surfaces are drawn together in the reduced Brillouin zone for the $\sqrt{2}\times\sqrt{2}$ supercell. LaFeSbO shows an enhanced nesting between the electron and hole surfaces which coincide with each other very isotropically with almost circular shapes compared with LaFeAsO.[34] For $BaFe_2Pn_2$, the arsenide exhibits a moderate nesting feature, while nesting looks poor for the antimonide because hole surfaces, which are present in the arsenide, are missing so that the electron surfaces have no hole surfaces to couple with nearby. LiFeSb also shows an inefficient nesting compared with LiFeAs with some hole surfaces missing around the Γ point.

The nesting feature can be more quantitatively estimated by evaluating the Pauli susceptibility $\chi_0(\mathbf{q})$ as a function of the momentum $\mathbf{q}$ in the static limit with matrix elements ignored. The result is displayed in Fig. 2. For LaFePnO, χ_0 is larger for LaFeSbO for entire range of $\mathbf{q}$, especially at the nesting vector $\mathbf{q}=(\pi,\pi)$ where the pronounced peak is located. This peak indicates the enhanced FS nesting for LaFeSbO, consistently with the FS topology in Fig. 1. For $BaFe_2Pn_2$, situation is drastically different. Although the sus-

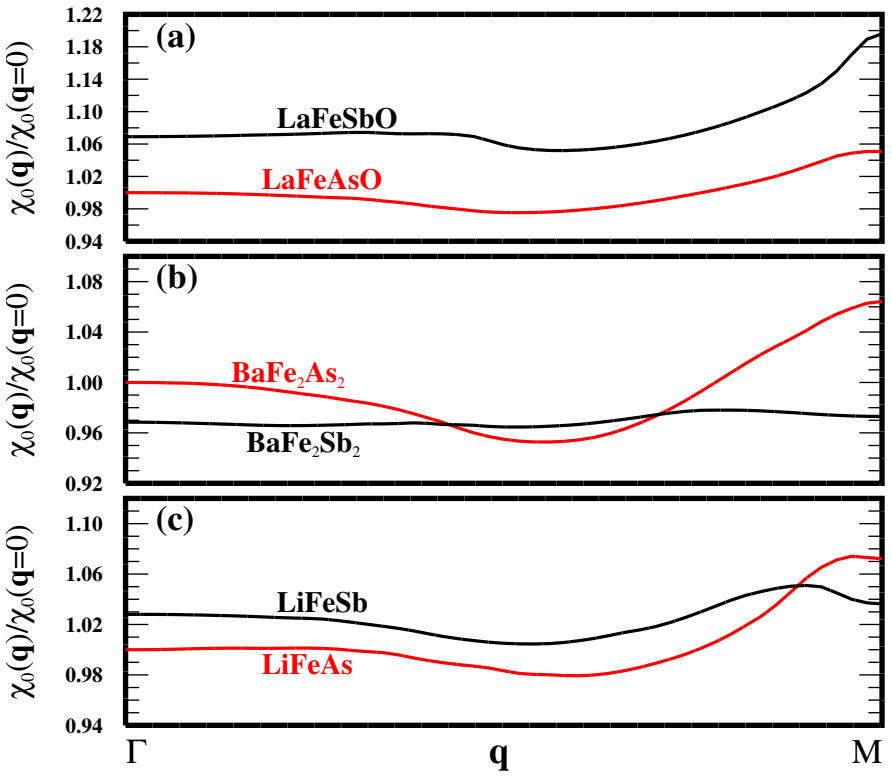

FIG. 2. (Color online) Pauli susceptibility $\chi_0(\mathbf{q})$ for (a) LaFePnO, (b) $BaFe_2Pn_2$, and (c) LiFePn, normalized by $\chi_0[\mathbf{q}=(0,0)]$ of the arsenide for each type of compounds.

ceptibility for $BaFe_2As_2$ has similar $\mathbf{q}$ dependence with those for LaFePnO, the susceptibility for $BaFe_2Sb_2$ is larger only for partial range of $\mathbf{q}$ with very weak $\mathbf{q}$ dependence and moreover there is no peak at $\mathbf{q}=(\pi,\pi)$. This feature clearly reflects the poor FS nesting in $BaFe_2Sb_2$ due to the lack of hole surfaces, as shown in Fig. 1. Finally, LiFeSb also has smaller $\chi_0(\mathbf{q})$ than LiFeAs near (π,π), hence LiFeSb has less effective FS nesting at (π,π) than LiFeAs.

Although many previous studies suggest the itinerant magnetism in iron pnictides that the stripe-type AFM is the SDW-type driven by the FS nesting, our results are in contradiction with this picture of magnetism. As we have just discussed, the FS nesting for $\mathbf{q}=(\pi,\pi)$, at which the stripe-type AFM occurs, is more pronounced for LaFeSbO than LaFeAsO, while $BaFe_2As_2$ and LiFeAs have more effective nesting feature than $BaFe_2Sb_2$ and LiFeSb, respectively. Thus, there is no universal trend in the FS nesting feature between arsenides and antimonides, which is in contrast, however, with the result that magnetism is stronger for antimonides than the respective arsenides for all three types of iron pnictides, with larger energy differences between AFM and NM states and greater Fe local magnetic moments for antimonides. This implies that the contribution of itinerant electrons to the magnetic energy and moment is relatively small.

IV. RELEVANCE OF THE HEISENBERG-TYPE LOCAL-MOMENT INTERACTION

In order to obtain a deeper insight into the nature of magnetism in these compounds, we consider another type of AFM ordering to examine how the relative stability and magnetic moments are affected by different AFM ordering. The additional AFM ordering considered is a "checkerboard-type" AFM ordering in which the four NN Fe atoms have the opposite spin direction to the Fe atom which they surround. This AFM ordering is denoted by AFM1 in this paper and the stripe-type AFM ordering by AFM2. In Table II, the relative energy of each AFM type and the magnetic moment on a Fe atom are listed for all the six compounds. For each compound, atomic structures optimized in the NM phase are used for all magnetic phases to see purely electronic contribution to the total-energy differences among magnetic phases without structural relaxation effects.

As shown in Table II, AFM1 is more stable than NM phase for all of the compounds and the stability and the Fe local magnetic moment are larger for the antimonides than their respective arsenides. Since the AFM1 ordering is surely not related to the FS nesting, there should be a mechanism other than the simple itinerant magnetism to explain the sta-

TABLE II. Stability of magnetic phases and Fe magnetic moments m in μ_B for iron pnictides. For each compound, calculations are done in the optimized structure for the NM phase. E_1 is the energy of AFM1 relative to the NM phases and E_2 is the energy of AFM2 relative to the AFM1 phases in meV per Fe atom.

Compound	E_1	m (AFM1)	E_2	m (AFM2)
LaFeAsO	−123	2.23	−109	2.35
LaFeSbO	−387	2.88	−136	2.83
$BaFe_2As_2$	−108	2.09	−64	2.20
$BaFe_2Sb_2$	−426	2.80	−75	2.78
LiFeAs	−45	1.83	−99	1.96
LiFeAs	−269	2.54	−118	2.63

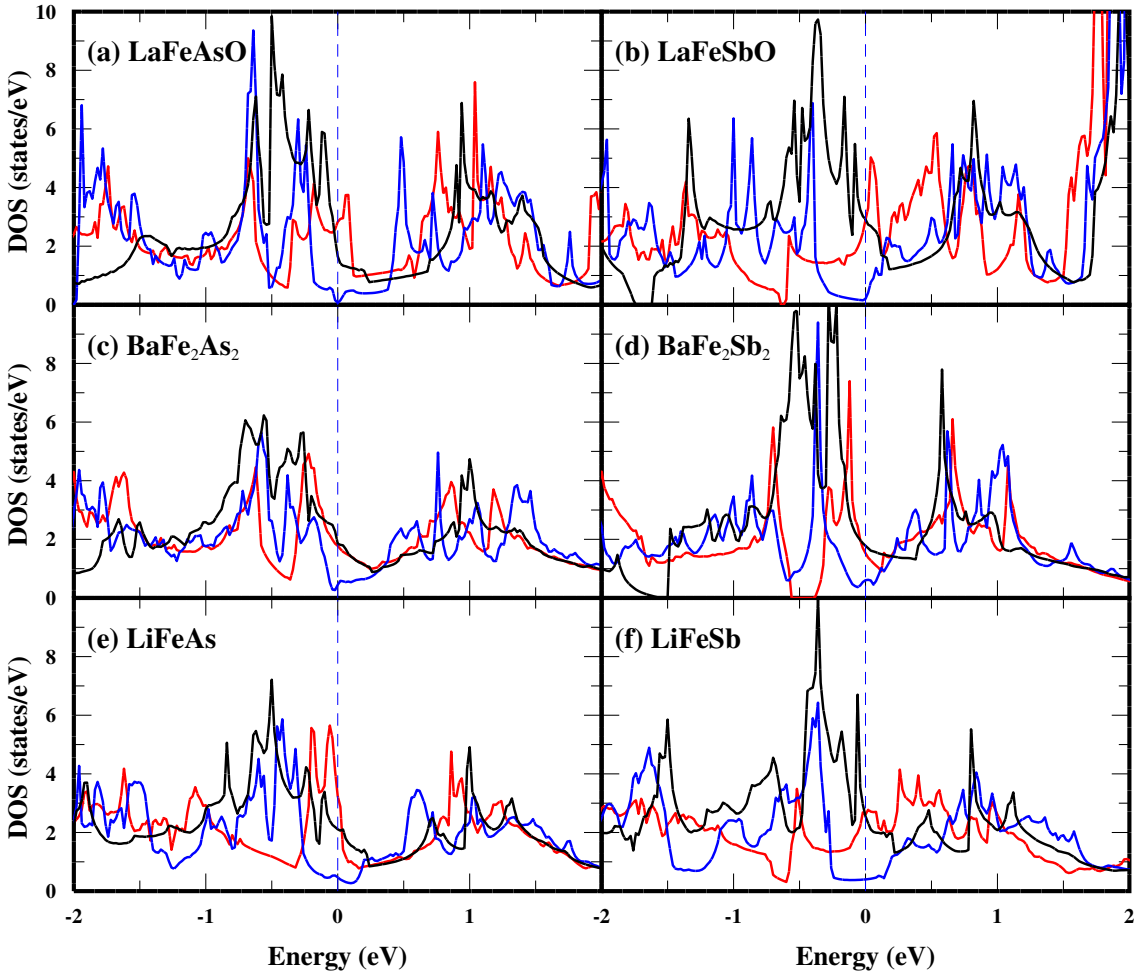

FIG. 3. (Color online) DOSs of (a) LaFeAsO, (b) LaFeSbO, (c) $BaFe_2As_2$, (d) $BaFe_2Sb_2$, (e) LiFeAs, and (f) LiFeSb calculated in the NM, AFM1, and AFM2 phases, which are shown in black, red (gray), and blue (dark gray), respectively.

bility of AFM1 and its enhancement in antimonides. Furthermore, we find energetic stability of AFM2 relative to AFM1 phases and magnetic moment in AFM2 phase are enhanced in all antimonides compared with respective arsenides, as shown in Table II. This is again in contradiction with FS nesting features related to the itinerant magnetism. On the contrary, the Heisenberg-type magnetic interaction picture can naturally account for our calculated magnetic properties of these materials. As the lattice parameters are larger for antimonides than their corresponding arsenides, the Fe $3d$ orbitals are more localized as is evident from the reduced band width around E_F.[34] Then consequently enhanced Hund's rule coupling along with the reduced crystal-field splitting among Fe d orbitals favors higher spin states of electrons in antimonides, as is in Table II. The importance of Hund's rule coupling and local nature of Fe magnetic moments in iron-based superconductors are also discussed in recently published theoretical works.[33,39–41]

The generally larger Fe magnetic moments in iron antimonides than in arsenides can explain the enhanced stability of AFM1 with respect to the NM phase, and AFM2 with respect to AFM1, for antimonides compared with arsenides within the Heisenberg interaction with $J_2 > J_1/2$.[27–29] To check further the validity of the Heisenberg Hamiltonian in capturing important total-energy contributions, we estimated the J_1 and J_2 with the total energies of three different magnetic orderings, the ferromagnetic ordering, AFM1, and another magnetic ordering where one spin is down and the other three spins are up in the $\sqrt{2}\times\sqrt{2}$ supercell containing four Fe atoms. Then the relative stability of AFM2 phase estimated with these exchange parameters and Heisenberg Hamiltonian is consistent with our actual total-energy results (shown in Table II) within about 60 meV per Fe atom.

V. FERMI-SURFACE RECONSTRUCTION IN THE AFM2 PHASE

While the magnetic ordering is determined by the Heisenberg-type local-moment interaction, a characteristic feature of the itinerant magnetism is also present in the AFM2 phase: there is clear difference in DOS between AFM2 and other phases calculated with the same structural parameters optimized for the NM phase for each compound, as displayed in Fig. 3. The NM phase has a finite DOS at E_F, and AFM1 magnetic ordering does not reduce the DOS at E_F, while it is greatly reduced for the AFM2 ordering. This feature indicates that the AFM2 phase involves the ordering-induced FS reconstruction by the coupling between the elec-

tron and hole surfaces, in contrast to the AFM1 phase where only the local magnetic interaction is involved. Our result qualitatively agrees with the recently suggested model[32] in which the itinerant electrons couple to the local magnetic moments which are AFM ordered. Even in the case of $BaFe_2Sb_2$, where the FS nesting is very ineffective as in Figs. 1 and 2, the AFM2 ordering produces the strong perturbing potential for the electron and hole bands to be hybridized, resulting in the partial gap in DOS at E_F, as shown in Fig. 3(d). Other compounds exhibit similar feature in DOS at E_F among different magnetic phases, indicating that the presence of partial gap is not sensitive to the detailed FS nesting characteristics as it is an induced feature by coupling to more robust underlying magnetism of the local-moment interaction.

VI. SUMMARY

In this work, we investigate the magnetic properties of known and hypothetical iron pnictides by the total-energy calculations. We find that our calculated FS nesting feature in the NM phase is not consistent with the trend of the magnetic stability that the AFM phases are more stable in antimonides than in arsenides. Heisenberg-type local-moment interaction is more appropriate to understand the energetics when we consider the larger Fe spin moment found in antimonides. Thus our results indicate that experimentally observed stripe-type AFM in iron pnictides is mainly driven by local-moment interaction while the reconstruction of Fermi surfaces and the partial gap at E_F emerge as an induced order by coupling to the local moments.

ACKNOWLEDGMENTS

This work was supported by the KRF (Grant No. KRF-2007-314-C00075) and by the KOSEF under Grant No. R01-2007-000-20922-0. Computational resources have been provided by KISTI Supercomputing Center (Project No. KSC-2008-S02-0004).

*h.j.choi@yonsei.ac.kr

[1] Y. Kamihara, H. Hiramatsu, M. Hirano, R. Kawamura, H. Yanagi, T. Kamiya, and H. Hosono, J. Am. Chem. Soc. **128**, 10012 (2006).
[2] Y. Kamihara, T. Watanabe, M. Hirano, and H. Hosono, J. Am. Chem. Soc. **130**, 3296 (2008).
[3] H. Takahashi, K. Igawa, K. Arii, Y. Kamihara, M. Hirano, and H. Hosono, Nature (London) **453**, 376 (2008).
[4] Z.-A. Ren, W. Lu, J. Yang, W. Yi, X.-L. Shen, Z.-C. Li, G.-C. Che, X.-L. Dong, L.-L. Sun, F. Zhou, and Z.-X. Zhao, Chin. Phys. Lett. **25**, 2215 (2008).
[5] M. Rotter, M. Tegel, D. Johrendt, I. Schellenberg, W. Hermes, and R. Pottgen, Phys. Rev. B **78**, 020503(R) (2008).
[6] M. Rotter, M. Tegel, and D. Johrendt, Phys. Rev. Lett. **101**, 107006 (2008).
[7] C. Krellner, N. Caroca-Canales, A. Jesche, H. Rosner, A. Ormeci, and C. Geibel, Phys. Rev. B **78**, 100504(R) (2008).
[8] G.-F. Chen, Z. Li, G. Li, W.-Z. Hu, J. Dong, J. Zhou, X.-D. Zhang, P. Zheng, N.-L. Wang, and J.-L. Luo, Chin. Phys. Lett. **25**, 3403 (2008).
[9] M. J. Pitcher, D. R. Parker, P. Adamson, S. J. C. Herkelrath, A. T. Boothroyd, R. M. Ibberson, M. Brunelli, and S. J. Clarke, Chem. Commun. (Cambridge) **2008**, 5918.
[10] X. C. Wang, Q. Q. Liu, Y. X. Lv, W. B. Gao, L. X. Yang, R. C. Yu, F. Y. Li, and C. Q. Jin, Solid State Commun. **148**, 538 (2008).
[11] J. H. Tapp, Z. Tang, B. Lv, K. Sasmal, B. Lorenz, P. C. W. Chu, and A. M. Guloy, Phys. Rev. B **78**, 060505(R) (2008).
[12] G. Giovannetti, S. Kumar, and J. van den Brink, Physica B (Amsterdam) **403**, 3653 (2008).
[13] D. J. Singh and M.-H. Du, Phys. Rev. Lett. **100**, 237003 (2008).
[14] K. Haule, J. H. Shim, and G. Kotliar, Phys. Rev. Lett. **100**, 226402 (2008).
[15] G. Xu, W. Ming, Y. Yao, X. Dai, S. Zhang, and Z. Fang, EPL **82**, 67002 (2008).
[16] I. I. Mazin, M. D. Johannes, L. Boeri, K. Koepernik, and D. J. Singh, Phys. Rev. B **78**, 085104 (2008).
[17] I. I. Mazin, D. J. Singh, M. D. Johannes, and M. H. Du, Phys. Rev. Lett. **101**, 057003 (2008).
[18] K. Kuroki, S. Onari, R. Arita, H. Usui, Y. Tanaka, H. Kontani, and H. Aoki, Phys. Rev. Lett. **101**, 087004 (2008).
[19] M. M. Korshunov and I. Eremin, Phys. Rev. B **78**, 140509(R) (2008).
[20] V. Cvetkovic and Z. Tesanovic, EPL **85**, 37002 (2009).
[21] Z. P. Yin, S. Lebegue, M. J. Han, B. P. Neal, S. Y. Savrasov, and W. E. Pickett, Phys. Rev. Lett. **101**, 047001 (2008).
[22] J. Dong, H. J. Zhang, G. Xu, Z. Li, G. Li, W. Z. Hu, D. Wu, G. F. Chen, X. Dai, J. L. Luo, Z. Fang, and N. L. Wang, EPL **83**, 27006 (2008).
[23] B. Lorenz, K. Sasmal, R. P. Chaudhury, X. H. Chen, R. H. Liu, T. Wu, and C. W. Chu, Phys. Rev. B **78**, 012505 (2008).
[24] C. de la Cruz, Q. Huang, J. W. Lynn, J. Li, W. Ratcliff II, J. L. Zarestky, H. A. Mook, G. F. Chen, J. L. Luo, N. L. Wang, and P. Dai, Nature (London) **453**, 899 (2008).
[25] H.-H. Klauss, H. Luetkens, R. Klingeler, C. Hess, F. J. Litterst, M. Kraken, M. M. Korshunov, I. Eremin, S.-L. Drechsler, R. Khasanov, A. Amato, J. Hamann-Borrero, N. Leps, A. Kondrat, G. Behr, J. Werner, and B. Buchner, Phys. Rev. Lett. **101**, 077005 (2008).
[26] W. Z. Hu, J. Dong, G. Li, Z. Li, P. Zheng, G. F. Chen, J. L. Luo, and N. L. Wang, Phys. Rev. Lett. **101**, 257005 (2008).
[27] Q. Si and E. Abrahams, Phys. Rev. Lett. **101**, 076401 (2008).
[28] L. X. Yang, Y. Zhang, H. W. Ou, J. F. Zhao, D. W. Shen, B. Zhou, J. Wei, F. Chen, M. Xu, C. He, Y. Chen, Z. D. Wang, X. F. Wang, T. Wu, G. Wu, X. H. Chen, M. Arita, K. Shimada, M. Taniguchi, Z. Y. Lu, T. Xiang, and D. L. Feng, Phys. Rev. Lett. **102**, 107002 (2009).
[29] T. Yildirim, Phys. Rev. Lett. **101**, 057010 (2008).
[30] J. Wu, P. Phillips, and A. H. Castro Neto, Phys. Rev. Lett. **101**, 126401 (2008).

[31] J. Wu and P. Phillips, arXiv:0901.3538 (unpublished).
[32] S.-P. Kou, T. Li, and Z.-Y. Weng, arXiv:0811.4111 (unpublished).
[33] G. D. Samolyuk and V. P. Antropov, Phys. Rev. B **79**, 052505 (2009).
[34] C.-Y. Moon, S. Y. Park, and H. J. Choi, Phys. Rev. B **78**, 212507 (2008).
[35] L. Zhang, A. Subedi, D. J. Singh, and M. H. Du, Phys. Rev. B **78**, 174520 (2008).
[36] J. P. Perdew, K. Burke, and M. Ernzerhof, Phys. Rev. Lett. **77**, 3865 (1996).
[37] D. Sanchez-Portal, P. Ordejon, E. Artacho, and J. M. Soler, Int. J. Quantum Chem. **65**, 453 (1997).
[38] H. J. Monkhorst and J. D. Pack, Phys. Rev. B **13**, 5188 (1976).
[39] J. Zhang, R. Sknepnek, R. M. Fernandes, and J. Schmalian, Phys. Rev. B **79**, 220502(R) (2009).
[40] E. Manousakis, Phys. Rev. B **79**, 220509(R) (2009).
[41] M. D. Johannes and I. I. Mazin, Phys. Rev. B **79**, 220510(R) (2009).